

Energy analysis of the cryogenic CO₂ capture process based on Stirling coolers

Chunfeng Song ^{a,*}, Yutaka Kitamura ^b, Shuhong Li ^b

^a *Collaborative Research Center for Energy Engineering, Institute of Industrial Science, The University of Tokyo, 4-6-1 Komaba, Meguro-Ku, Tokyo 153-8505, Japan*

^b *Graduate School of Life and Environmental Sciences, University of Tsukuba, 1-1-1, Tennodai, Tsukuba, Ibaraki 305-8572, Japan*

* Corresponding author. Tel.: +81-(0)3-5452-6898; Fax: +81-(0)3-5452-6728.

E-mail address: songcf@iis.u-tokyo.ac.jp

Abstract

In the existing coal-fired power plants, the energy penalty associated with CO₂ capture process is an important challenge. For this reason, energy analysis has been widely used as a powerful tool to optimize the capture efficiency and reduce energy consumption. In our previous work, a Stirling cooler based cryogenic CO₂ capture system was outlined. Process simulation and energy analysis of the system was undertaken in this research. The whole CO₂ capture process is composed of three sections; pre-chilling, CO₂ anti-sublimation and storage. The energy consumption of each section in the system was investigated in detail. The results show that when the flow rate of flue gas (13 vol.% CO₂) is set at 5 L/min and the temperature of Stirling cooler -1, 2 and 3 is set at -30, -120 and -120 °C, the energy consumption of the pre-chilling, CO₂ anti-sublimation and storage sections are 15.58_{thermal} J/s, 30.48_{thermal} J/s and 11.40_{thermal} J/s, respectively. The total energy consumption of the cryogenic CO₂ capture system is 57.46_{thermal} J/s (equal to 689.52 J/L flue gas).

Keywords: CO₂ capture, cryogenic, Stirling cooler, energy consumption

1. Introduction

At present, a number of large industrial power stations have become dominant greenhouse gas (GHG) emitters, and coal-fired power plants have been paid wide attention as one of the most important. According to World Energy Outlook 2009 of the International Energy Agency (IEA), by 2030 coal will account for approximately 44% of world energy consumption [1]. In the face of this situation, integration of CO₂ capture and storage (CCS) technologies into CO₂ emission sources is an effective strategy to mitigate increasing climate issues.

In recent decades, several CO₂ capture and storage technologies for post-combustion power plants such as solvent absorption, sorbent adsorption, membrane permeation and cryogenic fractionation have been developed [2]. Among these techniques, the chemical absorption method has been identified widely in research as the most mature technology, due to its significant advantage of being used for different CO₂ sources even for dilute CO₂ concentrations (3 vol.% for gas turbine) [3]. Adsorption is a promising alternative to the CO₂ absorption method. The main technologies are thermal (TSA), electrical (ESA) or pressure/vacuum (PSA/VSA) swing adsorption, which use solid adsorbents in a number of adsorption columns [4]. The common solid adsorbents are activated carbon, zeolite, CaO, etc [5]. Furthermore, application of the polymeric membrane on CO₂ separation has been widely investigated in recent years due to its significant characteristics (i.e. high selectivity and high driving force) [6]. Cryogenic fractionation is a well known technique for air

separation and also has been utilized in oxy-fuel combustion CO₂ capture processes [7,8]. The typical cryogenic CO₂ capture process contains single or twin column distillations, Ryan Holmes process, controlled freezing (Exxon) [9-11]. Compared to conventional low temperature processes, the Stirling cooler system can separate CO₂ from the diluted flue gas (typically 13% CO₂) and the capture process is implemented under atmosphere [12].

Although research in CO₂ capture technologies has made remarkable progress, the energy penalty for existing technologies is still high (around 50 \$ per ton of CO₂ avoided) [13]. The major challenge for existing CO₂ capture technologies is to lessen the energy consumption of the capital and operational costs. For the absorption and adsorption processes, a large amount of heat is required to regenerate the solvents and sorbents [14,15]. Membrane and cryogenic methods are more suitable for high CO₂ concentration sources. When the CO₂ is diluted in the flue gas (lower than 30 vol.%), the energy consumption of these processes will obviously increase [16,17]. Therefore, growing attention has been paid to energy reduction of CO₂ capture and storage technologies. For example, different chemical absorption process configurations have been investigated to reduce energy consumption [18,19]. Meanwhile, novel materials have been developed as absorbents and adsorbents to reduce the energy penalty of the absorption and adsorption processes [20]. In 2012, Luis et al. summarized the current situation of membrane CO₂ capture technologies [21]. As they pointed out, the existing permeation processes are still expensive and few membrane modules are

commercially available. In 2011, Tuinier et al. evaluated the energy consumption of a novel post-combustion CO₂ capture process based on cryogenic packed beds [17]. Their research indicated that 3.6 MJ electric energy (for per kg CO₂) would be consumed to generate the required refrigeration condition. In addition, previous research indicates that CO₂ capture is an intricate and integrated process, and various forms of energy are utilized [22]. Therefore, energy analysis of the capture process plays a significant role in the improvement of capture efficiency and the reduction of energy penalty.

In light of these concerns, efforts are implemented in energy analysis to reduce the energy penalty of CO₂ capture processes. The objective of the work is to simulate and analyze the energy efficiency of the cryogenic CO₂ system based on Stirling coolers (SCs). In order to achieve this aim, the detailed energy consumption of different stages in the process has been investigated under different conditions (e.g., flow rate of gas stream, temperature of Stirling cooler and CO₂ concentration).

The paper is structured as follows: Section 2 describes the base case of the cryogenic CO₂ capture process. Section 3 analyzes the overall energy demand of the process and simulates the thermodynamic characteristics of the cryogenic system. Section 4 introduces detailed simulation work and the typical parameters that influence the energy requirement of the system. Section 5 investigates the energy requirements of different stages in the system. Economic evaluation and comparison with other technologies are also carried out. Section 6 summarizes the main

conclusions and prospects for future work.

2. Base case description

The schematic for the anti-sublimation CO₂ capture process is shown in Fig. 1. The main part comprises the Stirling coolers (SCs), vacuum pump, freezing tower, camera, control panel and structure frame [23]. The whole process consists of 3 sections: 1) pre-chilling tower; 2) CO₂ anti-sublimation tower; 3) storage column.

2.1 Pre-chilling tower

Initially, the flue gas is pre-chilled by SC-1 in the pre-chilling tower. There are two important functions of the pre-chilling process. Firstly, the gas stream can be cooled down to a low temperature which is beneficial to improve the total CO₂ capture efficiency. Simultaneously, the pre-chilling process can effectively avoid the mechanical damage caused by a sharp temperature drop. Secondly, in the pre-chilling tower, the moisture in the feed gas condenses into water under low temperature conditions. Owing to the subsequent hot gas stream there is no ice generated during the whole process. The separated water flows out from the outlet to avoid clogging the vessel which is a key issue of the anti-sublimation separation technology. Meanwhile, the other gas flows into the CO₂ anti-sublimation tower.

2.2 CO₂ anti-sublimation tower

In the CO₂ anti-sublimation tower, SC-2 provides a cryogenic condition

(approximately $-110\text{ }^{\circ}\text{C}$), and the dry flue gas is chilled to below $-100\text{ }^{\circ}\text{C}$. According to the work of Clodic et al., the freezing point of CO_2 is related to its partial pressure in the gas mixture [24]. Fig. 2(a) shows the relationship between freezing point and CO_2 concentration. Typically for the flue gas (3~20 vol.% CO_2) in Fig. 2(b), the freezing point of CO_2 varies between $-112\text{ }^{\circ}\text{C}$ ~ $-97\text{ }^{\circ}\text{C}$. Therefore, under low temperature in the CO_2 anti-sublimation tower, CO_2 in the flue gas could solidify into dry ice and frost onto the heat exchanger of SC-2 immediately. In this way, the capture of CO_2 from the feed gas is realized. It should be pointed out that the frosted CO_2 on the heat exchanger of SC-2 will adversely affect the heat and mass transfer process. For this reason, a motor driven scraper is used to scrape the deposited CO_2 down to the storage column.

2.3 Storage column

The last step of the whole capture process is to gather the captured CO_2 by SC-3. In the previous section, by spinning the scraping rod on the heat exchanger of SC-2, dry ice falls down into the storage column. Meanwhile, SC-3 provides a low temperature condition (below $-78.5\text{ }^{\circ}\text{C}$) to store the dry ice and prevent it from gasifying. On the other hand, residual gas (such as N_2) exhausts from the gas outlet without phase change. The detailed CO_2 deposition and storage process is the system is shown in Fig. 3. As latent heat with deposited CO_2 is substantial, we added a heat exchanger between the subsequent stream and frosted the CO_2 to recover it.

2.4 Cryogenic performance of cryogenic CO₂ capture system

In order to understand the intricate CO₂ capture process better and improve the capture efficiency the cryogenic performances of the three stages in the system are outlined in this section. Some geometrical assumption is put forward to simplify the intricate process. The detail structure of the columns used in the system is depicted in Fig. 4. The geometric dimension of pre-chilling, CO₂ anti-sublimation and storage columns is listed in Table 1.

The distribution of temperature in the pre-chilling, CO₂ anti-sublimation and storage columns is simulated in Fig. 5. The temperature field of the three columns is labeled in the radial position. Because the function of the pre-chilling section is to reduce the temperature of feed gas and separate moisture, the lowest temperature is around -20 °C. By contrast, the minimum temperature in the CO₂ anti-sublimation tower can drop to -105 °C to anti-sublimate the CO₂ from the flue gas. For the storage column, for conditions below -78 °C (the frost point of the pure CO₂) must be maintained in order to avoid frosted CO₂ sublimation.

3. Theoretical analysis

3.1 Overall energy consumption of the process

The energy flow diagram of the cryogenic CO₂ capture process is shown in Fig. 6. First, the flue gas from the impurity removal units is introduced into the pre-chilling section. In the next stage, SC-1 provides cold energy (Q_{SC-1}) to the pre-chilling tower.

Under low temperature conditions, the moisture in the gas stream can be condensed into water and separated from the outlet of the condensate tube. Then, the treated gas is introduced into the CO₂ anti-sublimation column, which is chilled by SC-2. With the cold energy Q_{SC-2} , the CO₂ in the gas stream can anti-sublimate into solid form (namely, dry ice) on the surface of the cold head. Simultaneously, the residual gas (mainly as N₂) exhausts from the system without phase change. The fallen CO₂ droplets are gathered and preserved by the cold energy from SC-3 (Q_{SC-3}). Finally, the cold energy of the captured CO₂ is recovered by heat exchangers. The heat loss of transmission during the three stages is represented by q_1 , q_2 and q_3 , respectively. Meanwhile, the latent heat loss associated with condensate water, residual gas and captured CO₂ is represented by q_4 , q_5 and q_6 , respectively.

3.2 Characteristics of flue gas

The mass flow rate of the simulated flue gas (φ_M) can be calculated as follows:

$$\varphi_M = \varphi_V \cdot \rho_g \quad (1)$$

where φ_V is the mass and volume flow rates of the gas mixture. ρ_g is the density of gas mixture and can be calculated as follows:

$$\rho_g = \omega_{N_2} \cdot \rho_{N_2} + \omega_{CO_2} \cdot \rho_{CO_2} + \omega_{H_2O} \cdot \rho_{H_2O} \quad (2)$$

here, ω_{N_2} , ω_{CO_2} and ω_{H_2O} are the percentage of N₂, CO₂ and water vapor in the flue gas, respectively. ρ_{N_2} , ρ_{CO_2} and ρ_{H_2O} are the density of N₂, CO₂ and H₂O, respectively.

The average heat capacity of the gas mixture (C_g) is expressed as follows:

$$C_g = \omega_{N_2} \cdot C_{N_2} + \omega_{CO_2} \cdot C_{CO_2} + \omega_{H_2O} \cdot C_{H_2O} \quad (3)$$

here, C_{N_2} , C_{CO_2} and C_{H_2O} are the heat capacity of N_2 , CO_2 and water vapor, respectively.

3.3 Energy consumption of the pre-chilling column

The total energy consumption of the pre-chilling column (Q_I) can be calculated by the heat removal of SC-1 (H_{SC-1}).

$$Q_I = \frac{H_{SC-1}}{\eta_{SC-1}} \quad (4)$$

here η_{SC-1} is the coefficient of performance (COP) for SC-1.

The heat removal of SC-1 can be divided into two parts: sensible heat of gas stream (Q_{SI}) and latent heat of evaporation for water vapor (Q_{LI}). Hereinto, the sensible heat for SC-1 (Q_{SI}) can be calculated as follows:

$$Q_{SI} = \varphi_M \cdot C_g \cdot \Delta T_I \quad (5)$$

here ΔT_I is the temperature variation from the inlet to the outlet of the pre-chilling column.

The calculation method for the latent heat of the condensate water (Q_{LI}) is presented in Equation (6):

$$Q_{LI} = \varphi_{m_{H_2O}} \cdot H_{H_2O} \quad (6)$$

here, H_{H_2O} is the vaporization heat of H_2O . The mass flow rate of H_2O ($\varphi_{m_{H_2O}}$) can be calculated as follows:

$$\varphi_{m_{H_2O}} = \frac{\omega_{H_2O} \cdot \varphi_V \cdot M_{H_2O}}{V_M} \quad (7)$$

where M_{H_2O} is the mole mass of H_2O . Thus, the total energy consumption of the pre-chilling column (Q_1) can be calculated by the sum of the sensible heat and latent heat.

$$Q_1 = \frac{Q_{S1} + Q_{L1}}{\eta_{SC-1}} \quad (8)$$

3.4 Energy consumption of the CO_2 anti-sublimation column

For the CO_2 capture column, the total energy consumption (Q_2) can be expressed as:

$$Q_2 = \frac{H_{SC-2}}{\eta_{SC-2}} \quad (9)$$

where H_{SC-2} is the heat removal of SC-2. η_{SC-2} is the COP of SC-2.

The heat removal of SC-2 can be divided into the sensible heat of gas stream (Q_{S2}) and latent heat of anti-sublimation for CO_2 (Q_{L2}). The sensible heat (Q_{S2}) can be calculated as follows:

$$Q_{S2} = \varphi_M \cdot C_g \cdot \Delta T_2 \quad (10)$$

here, ΔT_2 is the temperature difference between the inlet and outlet of the CO_2 anti-sublimation column.

In addition, the latent heat (Q_{L2}) can be calculated as follows:

$$Q_{L2} = \varphi_{m_{CO_2}} \cdot H_{CO_2} \quad (11)$$

here, H_{CO_2} is the heat of sublimation for CO_2 . The mass flow rate of CO_2 ($\varphi_{m_{CO_2}}$)

can be calculated as follows:

$$\varphi_{m\ CO_2} = \frac{\omega_{CO_2} \cdot \varphi_V \cdot M_{CO_2}}{V_M} \quad (12)$$

The total energy consumption of the CO₂ anti-sublimation column (Q_2) is the sum of the sensible heat and latent heat:

$$Q_2 = \frac{Q_{S2} + Q_{L2}}{\eta_{SC-2}} \quad (13)$$

3.5 Energy consumption of the storage column

Due to no phase change in the storage column, the heat removal of SC-3 (H_{SC-3}) is mainly used to maintain the preserving condition to avoid the sublimation of captured CO₂.

$$H_{SC-3} = \varphi_{m\ CO_2} \cdot C_{CO_2} \cdot \Delta T_3 \quad (14)$$

Thus, the total energy consumption (Q_3) of the storage column can be calculated as follows:

$$Q_3 = \frac{\varphi_{m\ CO_2} \cdot C_{CO_2} \cdot \Delta T_3}{\eta_{SC-3}} \quad (15)$$

here η_{SC-3} is the COP of SC-3.

4. Methodology

4.1 Simulation work

The simulation work was undertaken by using a commercial process simulator (Aspen Plus software package, Version 7.3), Peng-Robinson equations of state are

reliable for three phase systems over a wide range of temperatures and pressures.

The condition of the flue gas is simulated as a typical coal-fired power plant and listed in Table 2. In order to improve the purity of CO₂ products and avoid corrosion of installation the impurities (i.e. SO_x, NO_x and ash) are often removed by the pre-treatment units, such as flue gas desulphurization (FGD), selective catalytic reduction (SCR) and electrostatic precipitators (ESP) [23]. In order to simplify the simulation process, these units are not considered in this work.

4.2 Parameter study

According to analysis in the previous section, it was found that there are three parameters (i.e., temperature of Stirling coolers, flow rate of flue gas and CO₂ concentration) that influence the energy consumption of the cryogenic system. The Stirling cooler 2 and 3 (SC-2 and 3) are used to capture and storage solid CO₂ in the whole process, and therefore their temperature is set at the minimum (-120 °C). The influence of temperature on the energy consumption of the system is considered SC-1 in this work. Meanwhile, the influence of the parameters on the energy consumption of the system is investigated at different levels.

The detailed conditions for the parameters are listed in Table 3. The performance of the SC is depicted in Table 4. In addition, the detailed characteristics of the feed gas (from a typical coal-fired power plant) have been introduced in our previous work [25].

5. Results and discussion

5.1 Effect of cryogenic temperature on SC-1

The relationship of energy consumption with the temperature on SC-1 is described in Fig. 7. The detailed energy variation of the different sections: (a) pre-chilling stage, (b) CO₂ anti-sublimation stage and (c) storage stage, according with the temperature of SC-1 is depicted in Fig. 8.

The results indicate that with decreasing temperature for SC-1, the energy consumption of pre-chilling (as shown in Fig. 8(a)) and the storage column (as shown in Fig. 8(c)) both increased. However, the energy consumption of the CO₂ anti-sublimation column (as shown in Fig. 8(b)) obviously decreased. When the temperature of SC-1 varied from -60 °C to -20 °C, the energy consumption of pre-chilling stage decreased from 18.78 to 14.50_{thermal} J/s, and the energy consumption of the storage column varied from 12.73 to 7.20_{thermal} J/s. In contrast, the energy consumption of the CO₂ anti-sublimation stage increased from 25.90 to 32.03_{thermal} J/s. This can be explained by the fact that sufficient pre-treatment in the pre-chilling tower is beneficial in decreasing the temperature of the flue gas, and part of the cold energy can be preserved in the CO₂ anti-sublimation stage. It can also be found that due to the flow rate and CO₂ concentration is constant, the variation of energy consumption for the system according to the temperature of SC-1 is modest.

5.2 Effect of the flow rate of gas stream

The energy consumption of the system under different flow rate of the gas stream is summarized in Fig. 9, and the detail of the energy variation of the three stages (pre-chilling, CO₂ anti-sublimation and storage) is shown in Fig. 10.

The results indicate that with an increase in the flow rate, the energy consumption of the pre-chilling column (as shown in Fig. 10 (a)) increased rapidly. When the flow rate was set at 1 L/min, the energy consumption of pre-chilling stage was 2.95_{thermal} J/s. When the flow rate increased to 5 L/min, the energy consumption of the pre-chilling stage increased to 15.58_{thermal} J/s. Meanwhile, the energy consumption of the CO₂ anti-sublimation column (as shown in Fig. 10 (b)) also increased according to the flow rate. When the flow rate increased from 1 to 5 L/min, the energy consumption of the CO₂ anti-sublimation stage varied from 6.18 to 30.48_{thermal} J/s. Finally, the energy consumption of the storage column (as shown in Fig. 10 (c)) also increased from 2.28 to 11.40_{thermal} J/s. The higher flow rate implies increasing demand on the treatment capacity. Therefore, more cold energy needs to be consumed to maintain the capture efficiency.

5.3 Effect of the CO₂ concentration

The energy variation of the whole cryogenic capture process with different CO₂ concentration is illustrated in Fig. 11. Meanwhile, the detailed variation of the energy consumption for the three stages according to the concentration of CO₂ in the gas stream is shown in Fig. 12.

The results indicate that with increasing CO₂ concentration, the energy consumption of the pre-chilling stage (as shown in Fig. 12 (a)) increased slowly. When the CO₂ concentration was set at 5 %, the energy consumption of the pre-chilling stage was 15.38_{thermal} J/s. When the CO₂ concentration increased to 40 %, the energy consumption of the pre-chilling stage increased to 16.38_{thermal} J/s. This is because the function of the pre-chilling stage is to separate the moisture from the flue gas. Therefore, the energy consumption of this part varied little with respect to the CO₂ concentration. By contrast, the energy consumption of the CO₂ anti-sublimation stage (as shown in Fig. 12 (b)) increased rapidly in association with the concentration of CO₂. When the concentration increased from 5 to 40 %, the energy consumption of the CO₂ anti-sublimation stage varied from 18.50 to 67.53_{thermal} J/s. Meanwhile, the energy consumption of the storage stage (as shown in Fig 12. (c)) also increased from 4.20 to 40.15_{thermal} J/s. As the CO₂ concentration increased, the requirement for phase change also increased. Thus, the energy consumption of the CO₂ anti-sublimation and storage stages increased rapidly.

5.4 Economic evaluation

The techno-economic evaluation (capital and operational cost) of the system is shown in Table 5. The total cost of the process consists of two parts: the capital cost and operational cost. The capital cost depends on the modules, including FPSCs, control panel and equipment frame. The capture process is carried out under the cryogenic conditions, therefore the operational cost of deposition is also an important

component and determined by the electric power consumption.

5.5 Comparison with existing processes

The boundary conditions of the different processes are summarized in Table 6, which indicates that the absorption, membrane and cryogenic factors (by Tuinier et al) are based on a 600 MWe coal fired power plant. By contrast, the cryogenic process developed by Clodic et al is tested in the pilot plant, and the adsorption process and present work are carried out on a laboratory scale.

The performance comparison among the existing CO₂ capture technologies is presented in Fig. 13. The comparison indicates that the cryogenic process exploited by Tuinier et al. is most costly (4.5 MJ_{thermal}/kg CO₂) compared with other technologies. This is because the cryogenic process is based on the consumption of electricity (approximately 1.8 MJ_{electrical}/kg CO₂), and which is equal to 4.5 MJ_{thermal}/kg CO₂ (the efficiency of conversion is around 0.4). By contrast, it can be seen that the present cryogenic process shows a promising CO₂ capture performance (1.37 MJ_{thermal} energy per capture of kg CO₂), and which is close to the performance of the most mature absorption process (about 1.6 MJ_{thermal}/kg CO₂). The low energy consumption of the present work can be attributed to the high efficiency of the SCs, which is higher than the conventional refrigerators. However, it should be pointed out that the performance of the exploited system has just been simulated, and this value should be further tested in a real power plant.

6. Conclusion

In this work, the overall energy flow of the Stirling cooler based cryogenic CO₂ capture process was simulated. The theoretical analysis of the energy consumption for each unit in the capture system was also undertaken. When the temperature of SC-1 varied from -20 to -60 °C, the total energy consumption of the cryogenic CO₂ capture system increased from 53.73 to 57.41_{thermal} J/s. When the flow rate of flue gas increased from 1 to 5 L/min, the total energy consumption of the cryogenic CO₂ capture system increased from 11.41 to 57.46_{thermal} J/s. When the CO₂ concentration in the flue gas increased from 5 % to 40 %, the total energy consumption of the cryogenic CO₂ capture system increased from 30.08 to 124.06_{thermal} J/s. The energy analysis provides a reliable way to improve capture efficiency and reduce energy penalty.

In future work, the dynamic operating process of system will be simulated, and simultaneously a pilot plant test based on the developed system will also be carried out. It should be noted that the sensible and latent heat of the separated components (such as condensate water and residual gas) is substantial. Therefore, the heat recovery units will be integrated into the system in the next step.

Acknowledgements

The authors acknowledge the funding provided by the Japan Science and Technology Agency (JST) for Transfer Program through the target driven R&D

(AS2115051D). We thank Mr. Yamano and Mr. Yamasaki of TANABE ENGINEERING for their help with fabrication.

Nomenclature

ΔT	Temperature, °C
C	Heat capacity, kJ/kg·°C
Q	Energy, J
q	Heat loss, J
H_{H_2O}	Heat of evaporation for water, kJ/mol
H_{CO_2}	Heat of sublimation for CO ₂ , kJ/mol
M	Mass, kg
V	Volume, L

Greek letters

ω_{H_2O}	Percentage of H ₂ O in flue gas, %
ω_{CO_2}	Percentage of CO ₂ in flue gas, %
φ	Flow rate, L/min
ρ	Density, kg/m ³
η	Coefficient of performance

Abbreviations

<i>CCS</i>	CO ₂ capture and storage
<i>GHG</i>	Greenhouse gas

<i>SC</i>	Stirling cooler
<i>EC</i>	Energy consumption
<i>TSA</i>	Temperature swing adsorption
<i>ESA</i>	Electric swing adsorption
<i>PSA</i>	Pressure swing adsorption
<i>VSA</i>	Vacuum swing adsorption
<i>COP</i>	Coefficient of performance

References

- [1] IEA. (International Energy Agency), 2009. World energy outlook. Paris France.
- [2] Rubin ES, Mantripragada H, Marks A, Versteeg P, Kitchin J. The outlook for improved carbon capture technology. *Prog. Energ. Combust.* 2012;38:630-71.
- [3] Olajire AA. CO₂ capture and separation technologies for end-of-pipe applications - A review. *Energy* 2010;35:2610-28.
- [4] Clausse M, Merel J, Meunier F. Numerical parametric study on CO₂ capture by indirect thermal swing adsorption. *Int. J. Greenhouse Gas Control.* 2011;5:1206-13.
- [5] Mondal MK, Balsora HK, Varshney P. Progress and trends in CO₂ capture/separation technologies: A review. *Energy* 2012;46:431-41.
- [6] Criscuoli A, Drioli E. New metrics for evaluating the performance of membrane operations in the logic of process intensification. *Ind Eng Chem Res.* 2007;46:2268-71.

- [7] Atsonios K, Panopoulos KD, Doukelis A, Koumanakos A, Kakaras E. Cryogenic method for H₂ and CH₄ recovery from a rich CO₂ stream in pre-combustion carbon capture and storage schemes. *Energy* 2013;53:106-13.
- [8] Cormos CC, Vatopoulos K, Tzimas E. Assessment of the consumption of water and construction materials in state-of-the-art fossil fuel power generation technologies involving CO₂ capture. *Energy* 2013;51:37-49.
- [9] Berstad D, Anantharaman R, Nekså P. Low-temperature CO₂ capture technologies – Applications and potential. *Int. J. Refrigeration* 2013;doi: 10.1016/j.ijrefrig.2013.03.017.
- [10] Holmes AS, Ryan JM. Distillative separations of gas mixtures containing methane. carbon dioxide and other components. 1984. US Patent 4,462,814.
- [11] Thomas ER, Denton RD. Conceptual Studies for CO₂/Natural Gas Separation Using the Controlled Freeze Zone (CFZ) Process. *Gas Separation and Purification*. 1988;2:84-9.
- [12] Song CF, Kitamura Y, Li SH, Ogasawara K. Design of a cryogenic CO₂ capture system based on Stirling coolers. *Int. J. Greenhouse Gas Control*. 2012;7:107-14.
- [13] Ho MT, Allinson GW, Wiley DE. Reducing the cost of CO₂ capture from flue gases using pressure swing adsorption. *Ind. Eng. Chem. Res.* 2008;47:4883-90.
- [14] Lund H, Mathiesen BV. The role of Carbon Capture and Storage in a future sustainable energy system. *Energy* 2012;44:469-76.
- [15] Li H, Ditaranto M, Yan J. Carbon capture with low energy penalty: Supplementary fired natural gas combined cycles. *Appl Energy* 2012;97:164–9.

- [16] M. Dios, J.A. Souto, J.J. Casares. Experimental development of CO₂, SO₂ and NO_x emission factors for mixed lignite and subbituminous coal-fired power plant. *Energy* 2013;53: 40-51.
- [17] Tuinier MJ, Hamers HP, Annaland MS. Techno-economic evaluation of cryogenic CO₂ capture — A comparison with absorption and membrane technology. *Int. J. Greenhouse Gas Control*. 2011;5:1559–65.
- [18] Ryi SK, Lee CB, Lee SW, Park JS. Pd-based composite membrane and its high-pressure module for pre-combustion CO₂ capture. *Energy* 2013;51:237-42
- [19] Moullec YL. Conceptual study of a high efficiency coal-fired power plant with CO₂ capture using a supercritical CO₂ Brayton cycle. *Energy* 2013;49:32-46.
- [20] Duan L, Huang K, Zhang X, Yang Y. Comparison study on different SOFC hybrid systems with zero-CO₂ emission. *Energy* 2013;58: 66-77
- [21] Luis P, Gerven TV, Bruggen BV. Recent developments in membrane-based technologies for CO₂ capture. *Prog. Energ. Combust.* 2012;38:419-48.
- [22] Iribarren D, Petrakopoulou F, Dufour J. Environmental and thermodynamic evaluation of CO₂ capture, transport and storage with and without enhanced resource recovery. *Energy* 2013;50:477-85.
- [23] Song CF, Kitamura Y, Li SH, Jiang WZ. Parametric analysis of a novel cryogenic CO₂ capture system based on Stirling coolers. *Environ. Sci. Technol.* 2012;46 (22):12735-41.
- [24] Clodic D, Younes M, Bill A. Test result of CO₂ capture by anti-sublimation capture efficiency and energy consumption for boiler plants. Seventh International Conference on Greenhouse Gas Control Technologies, GHGT7, Vancouver, Canada, 2004, 6-9 September.

- [25] Song CF, Kitamura Y, Li SH. Evaluation of Stirling cooler system for cryogenic CO₂ capture. *Appl Energy* 2012;98:491-501.
- [26] Ho MT, Allinson GW, Wiley DE. Comparison of MEA capture cost for low CO₂ emissions sources in Australia. *Int. J. Greenhouse Gas Control*. 2011;5:49-60.
- [27] Hussain A, Hägg MB. A feasibility study of CO₂ capture from flue gas by a facilitated transport membrane. *J. Membrane Sci.* 2010;359:140-48.

Figure captions

Fig. 1. Schematic of the developed anti-sublimation capture process.

Fig. 2. The relationship between freezing point ($^{\circ}\text{C}$) and CO_2 concentration (vol.%) (a); in the case of typical flue gas (b).

Fig. 3. The detailed CO_2 capture and storage stage in the system.

Fig. 4. The geometrical structure of the columns in the system.

Fig. 5. Temperature distributions in the pre-cooling tower, CO_2 anti-sublimation tower and storage column.

Fig. 6. The overall energy flow of the cryogenic CO_2 capture process.

Fig. 7. Influence of temperature of SC-1 on the energy consumption of the pre-chilling, CO_2 anti-sublimation and storage stages.

Fig. 8. Effect of the temperature of SC-1 on the energy consumption of the cryogenic CO_2 capture system. (a) Pre-chilling stage; (b) CO_2 anti-sublimation stage; (c) storage stage. The flow rate of the gas stream is set at 5 L/min. The temperature of SC-2 and 3 are both set at -120°C . The COP of SC-1, 2 and 3 are 1.1, 0.7 and 0.7, respectively. The concentration of CO_2 is set at 13% (in a typical the coal-fired power plant). The conversion efficiency from electric power to thermal energy is defined as 40%.

Fig. 9. Influence of flow rate on the energy consumption of the pre-chilling, CO₂ anti-sublimation and storage stages.

Fig. 10. Effect of flow rate on the energy consumption of the cryogenic CO₂ capture system. (a) Pre-chilling stage; (b) CO₂ anti-sublimation stage; (c) storage stage. The temperature of SC-1, 2 and 3 are set at -30°C, -120°C and -120°C, respectively. The COP of SC-1, 2 and 3 are 1.1, 0.7 and 0.7, respectively. The concentration of CO₂ is set at 13%. The conversion efficiency from electric power to thermal energy is defined as 40%.

Fig. 11. Influence of CO₂ concentration on the energy consumption of the pre-chilling, CO₂ anti-sublimation and storage stages.

Fig. 12. Effect of CO₂ concentration on the energy consumption of the cryogenic CO₂ capture system. (a) Pre-chilling stage; (b) CO₂ anti-sublimation stage; (c) storage stage. The temperature of SC-1, 2 and 3 are set at -30°C, -120°C and -120°C, respectively. The COP of SC-1, 2 and 3 are 1.1, 0.7 and 0.7, respectively. The flow rate of flue gas is set at 5 L/min. The conversion efficiency from electric power to thermal energy is defined as 40%.

Fig. 13. Comparison of the existing CO₂ capture technologies.

Fig. 14. Conceptual design of the scaled up cryogenic CO₂ capture process based Stirling coolers.

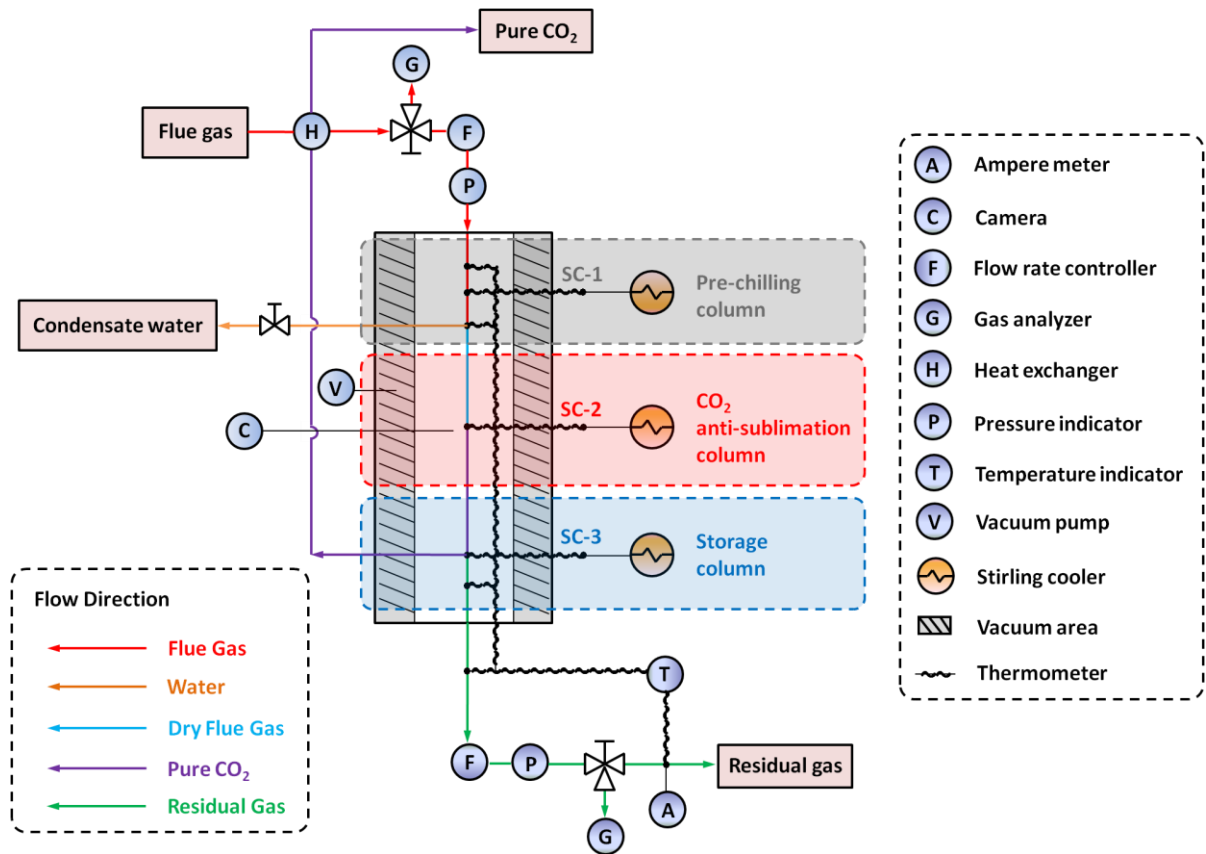
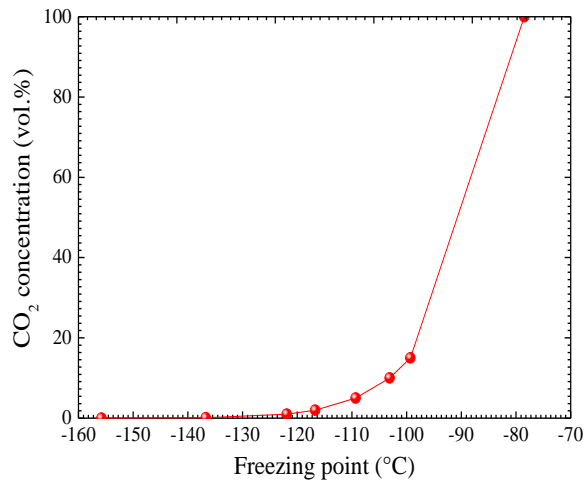
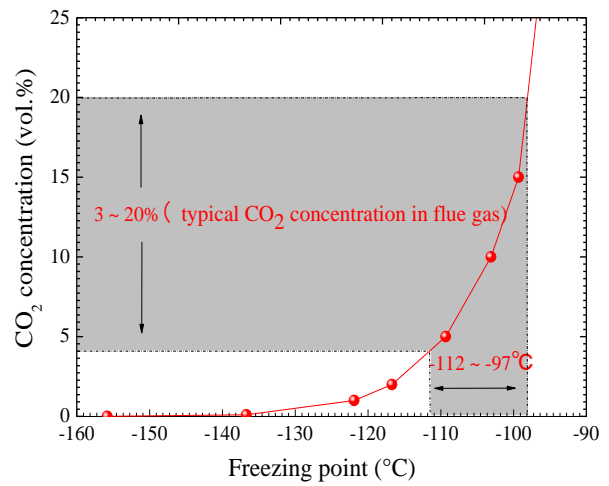


Fig. 1. Schematic of the developed anti-sublimation capture process.



(a)



(b)

Fig. 2. The relationship between freezing point (°C) and CO₂ concentration (vol.%) (a); in the case of typical flue gas (b).



(a)

(b)

Fig. 3. The detailed CO₂ capture and storage stage in the system.

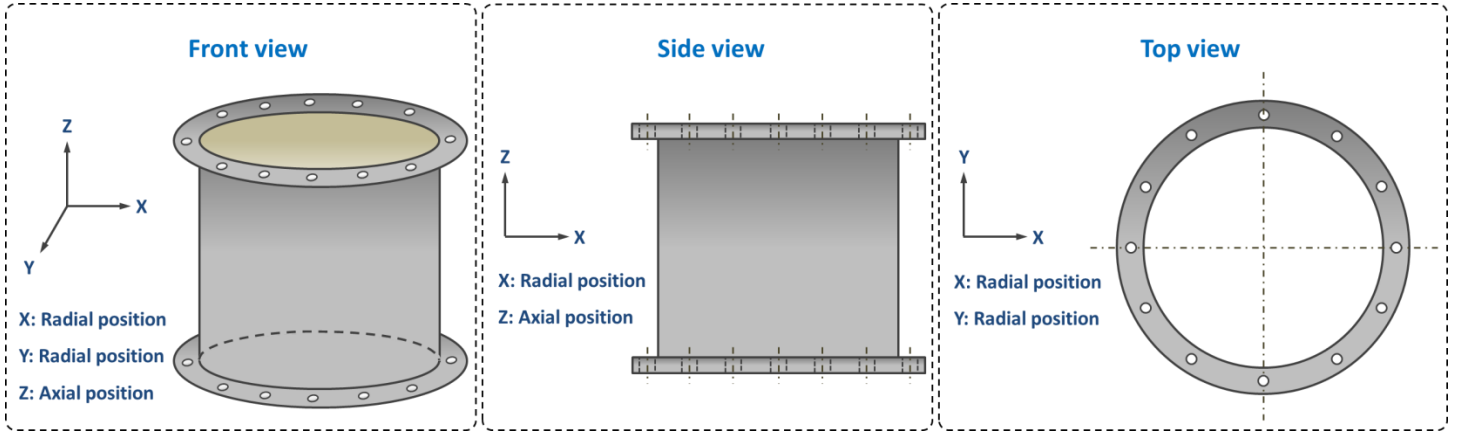


Fig. 4. The geometrical structure of the columns in the system.

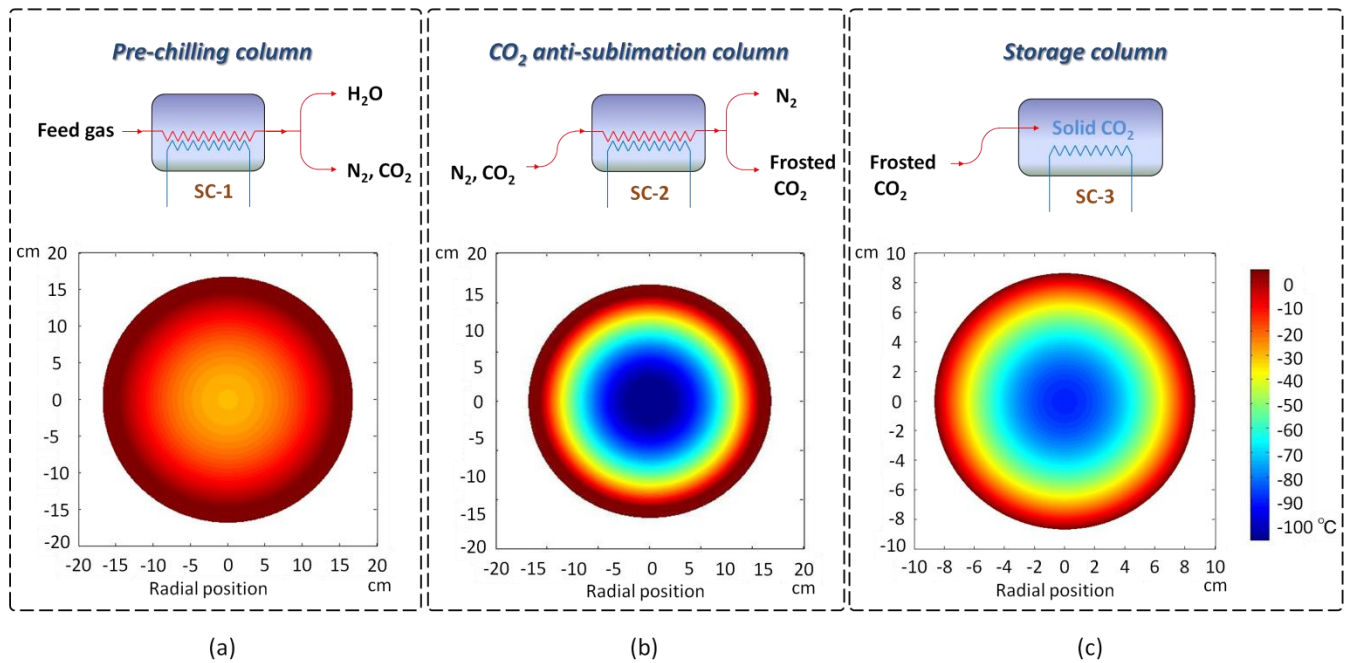


Fig. 5. Temperature distributions in the pre-cooling tower, CO₂ anti-sublimation tower and storage column.

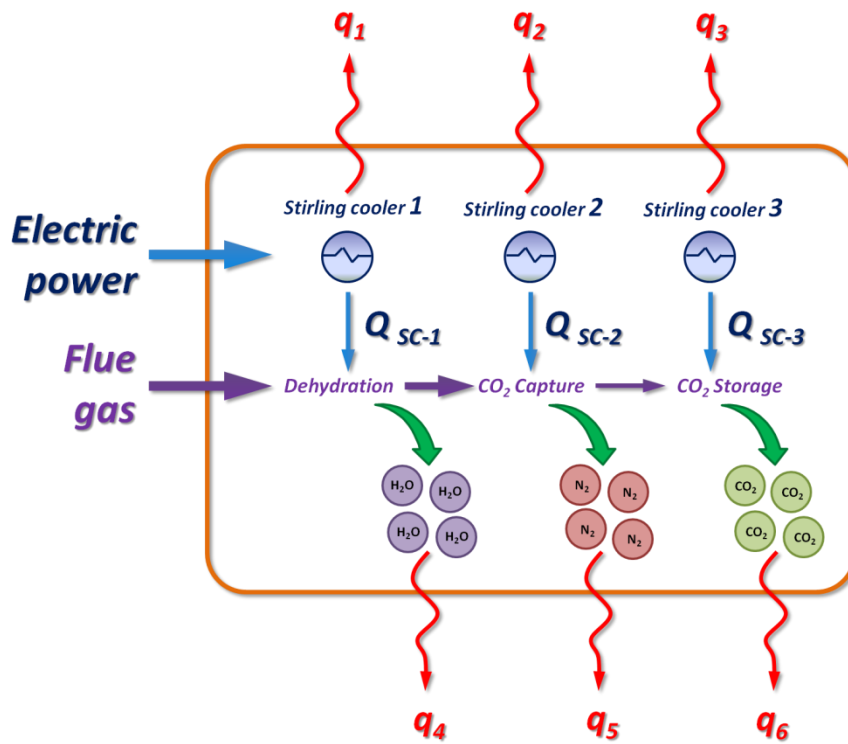


Fig. 6. The overall energy flow of the cryogenic CO₂ capture process.

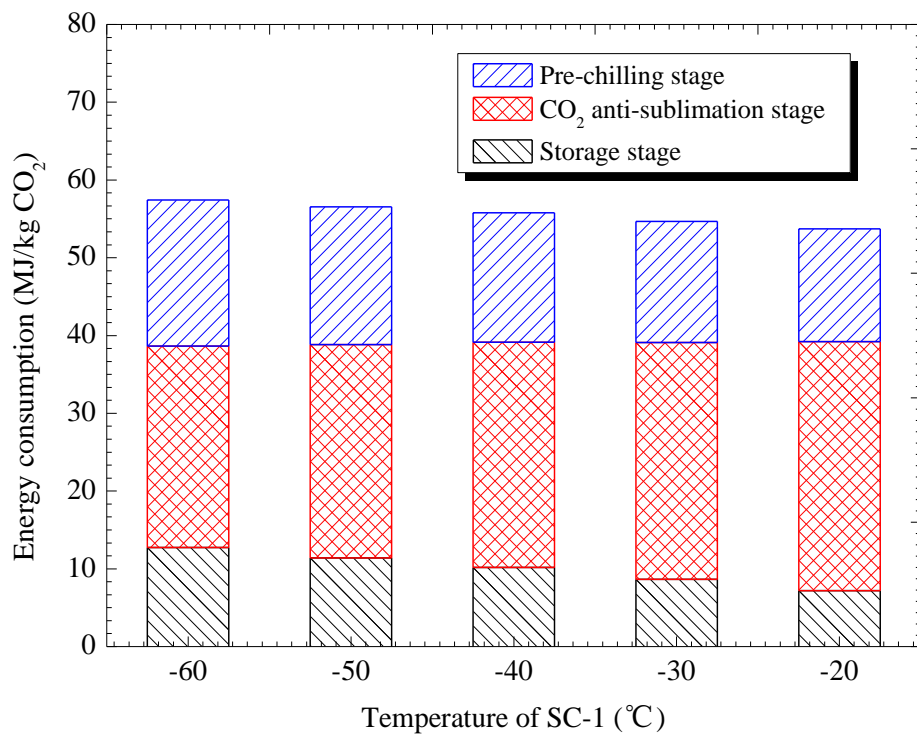
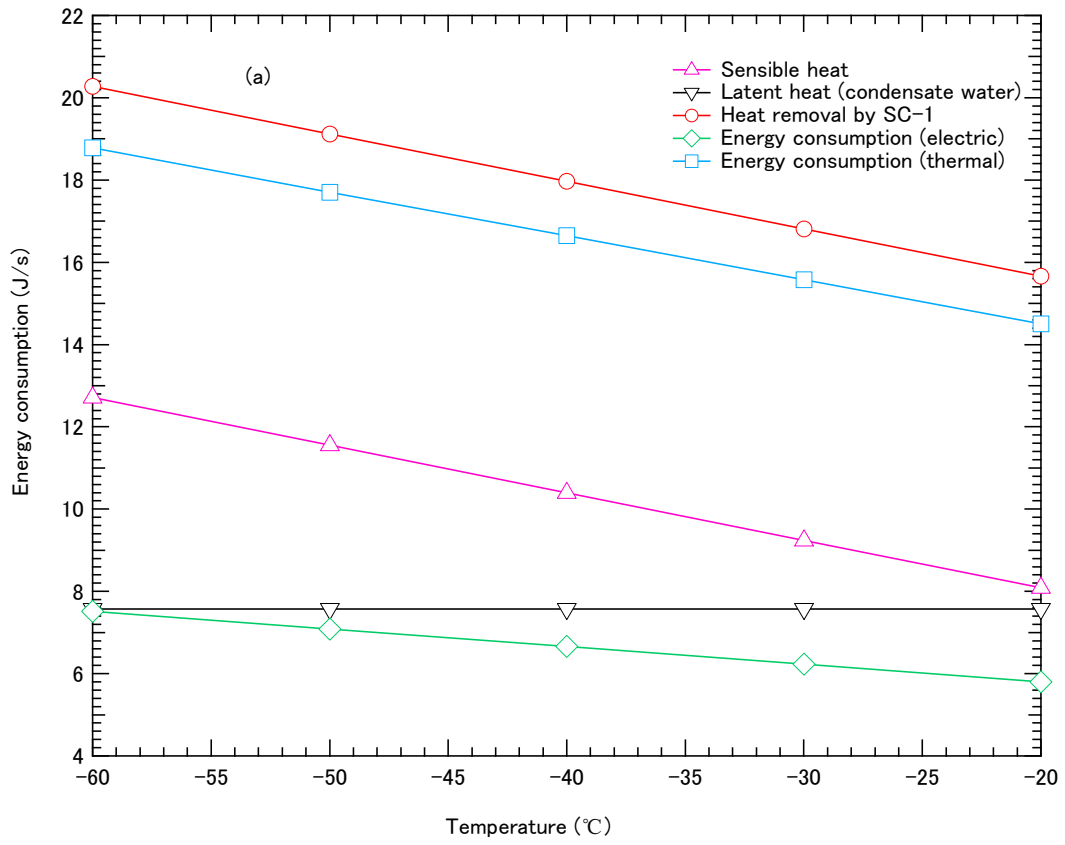


Fig. 7. Influence of temperature of SC-1 on the energy consumption of the pre-chilling, CO₂ anti-sublimation and storage stages.



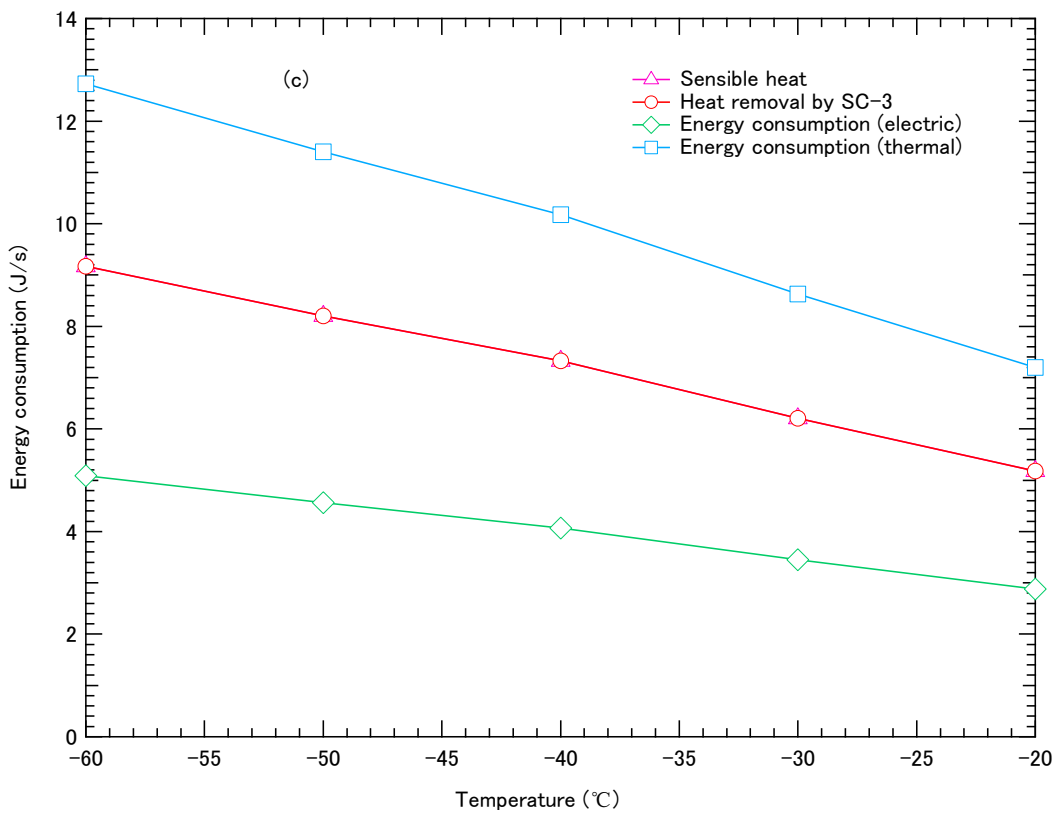
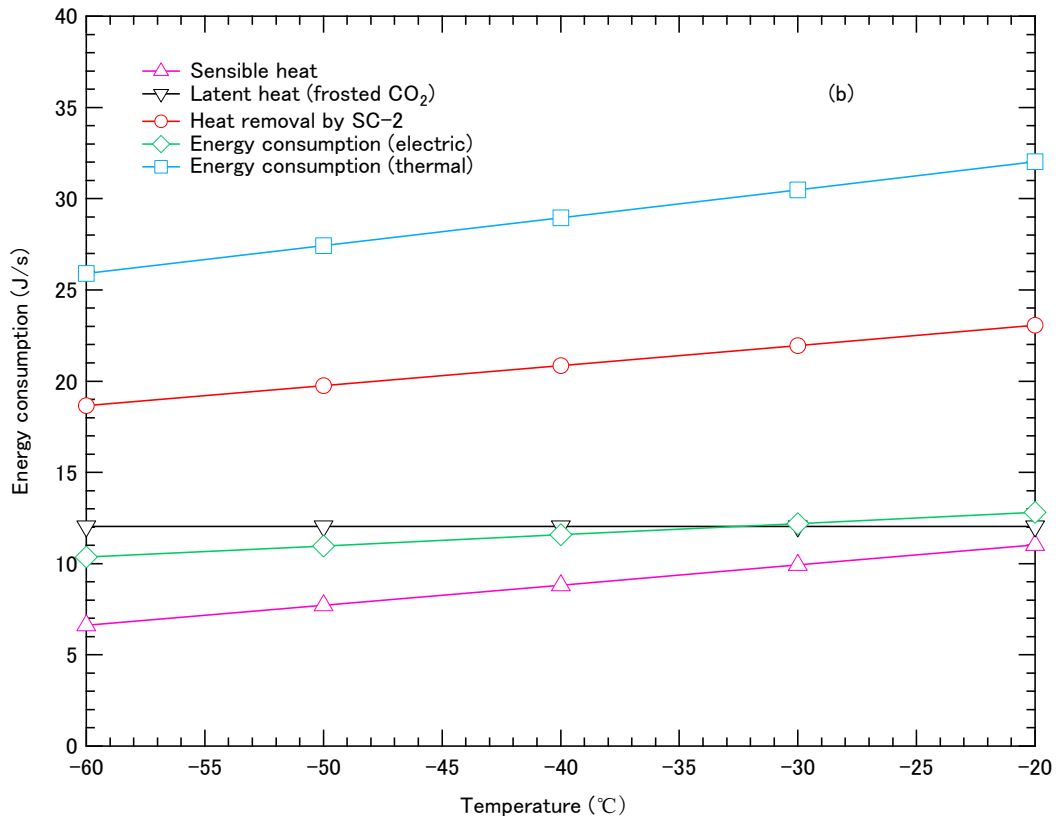


Fig. 8. Effect of the temperature of SC-1 on the energy consumption of the cryogenic CO₂ capture system. (a) Pre-chilling stage; (b) CO₂ anti-sublimation stage; (c) storage stage. The flow rate of the gas stream is set at 5 L/min. The temperature of SC-2 and 3 are both set at -120°C. The COP of SC-1, 2 and 3 are 1.1, 0.7 and 0.7, respectively. The concentration of CO₂ is set at 13% (in a typical the coal-fired power plant). The conversion efficiency from electric power to thermal energy is defined as 40%.

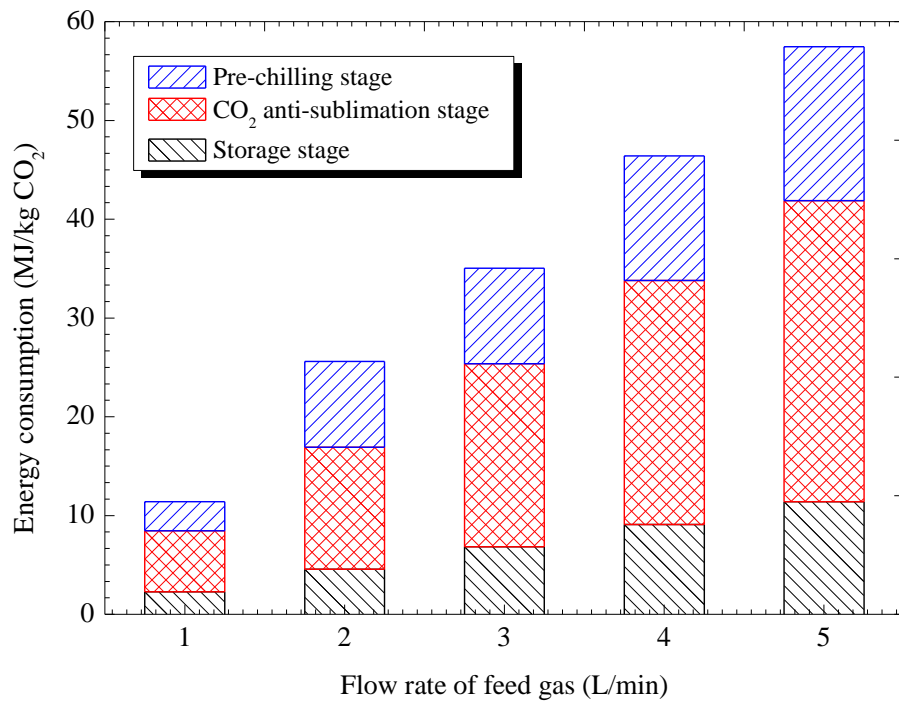
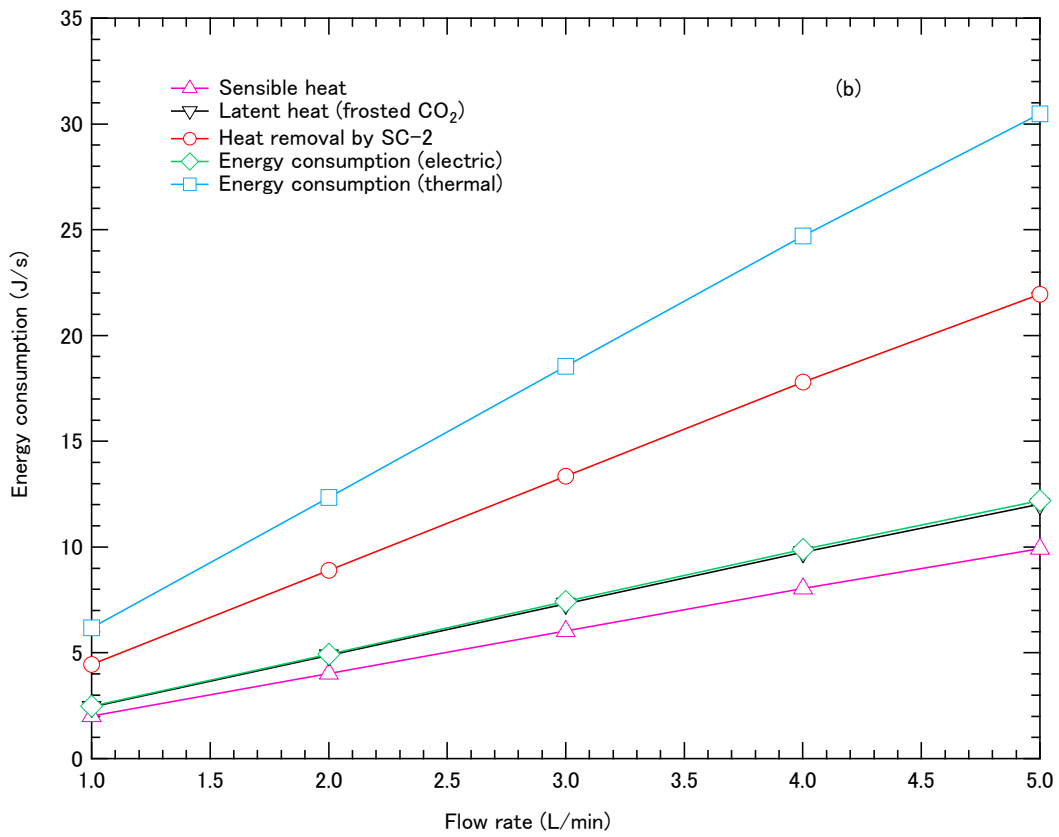
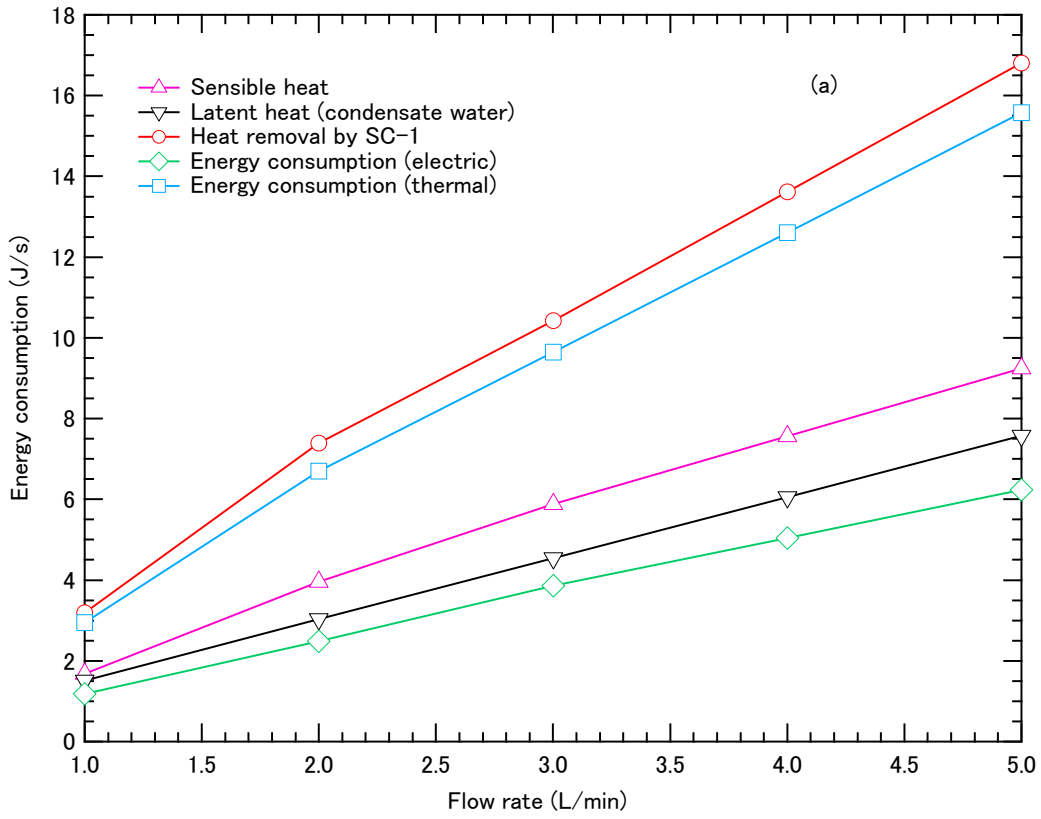


Fig. 9. Influence of flow rate on the energy consumption of the pre-chilling, CO₂ anti-sublimation and storage stages.



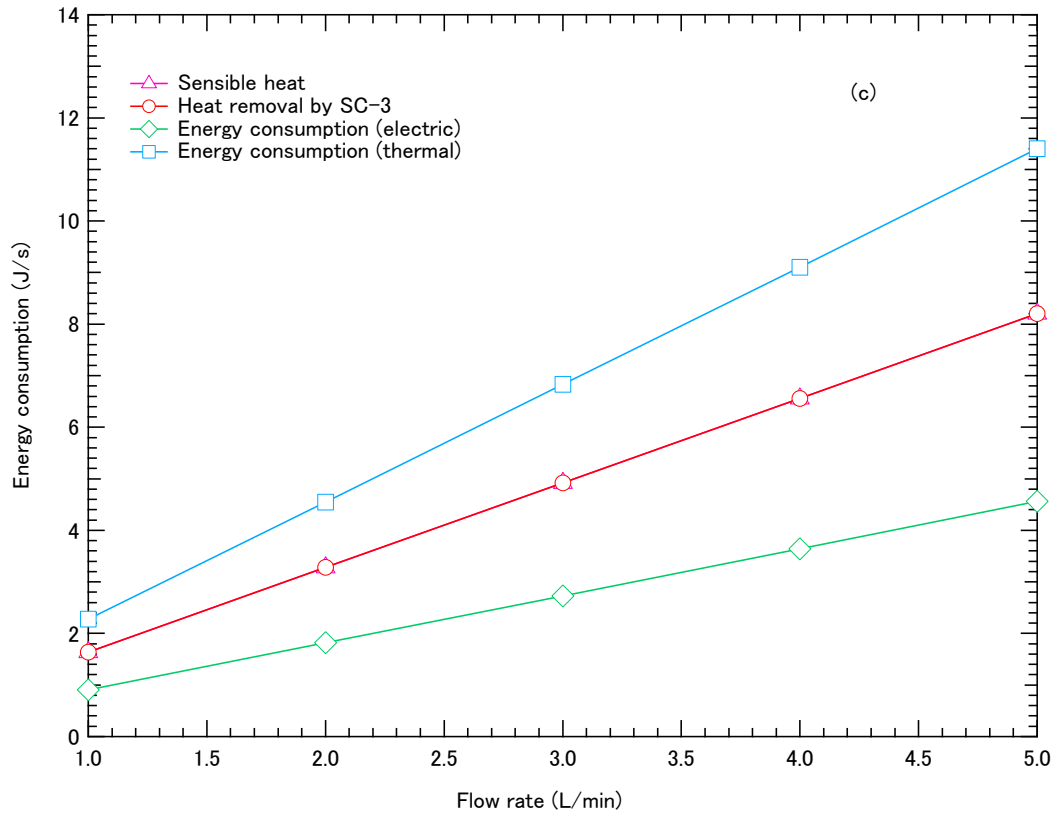


Fig. 10. Effect of flow rate on the energy consumption of the cryogenic CO₂ capture system. (a) Pre-chilling stage; (b) CO₂ anti-sublimation stage; (c) storage stage. The temperature of SC-1, 2 and 3 are set at -30°C, -120°C and -120°C, respectively. The COP of SC-1, 2 and 3 are 1.1, 0.7 and 0.7, respectively. The concentration of CO₂ is set at 13%. The conversion efficiency from electric power to thermal energy is defined as 40%.

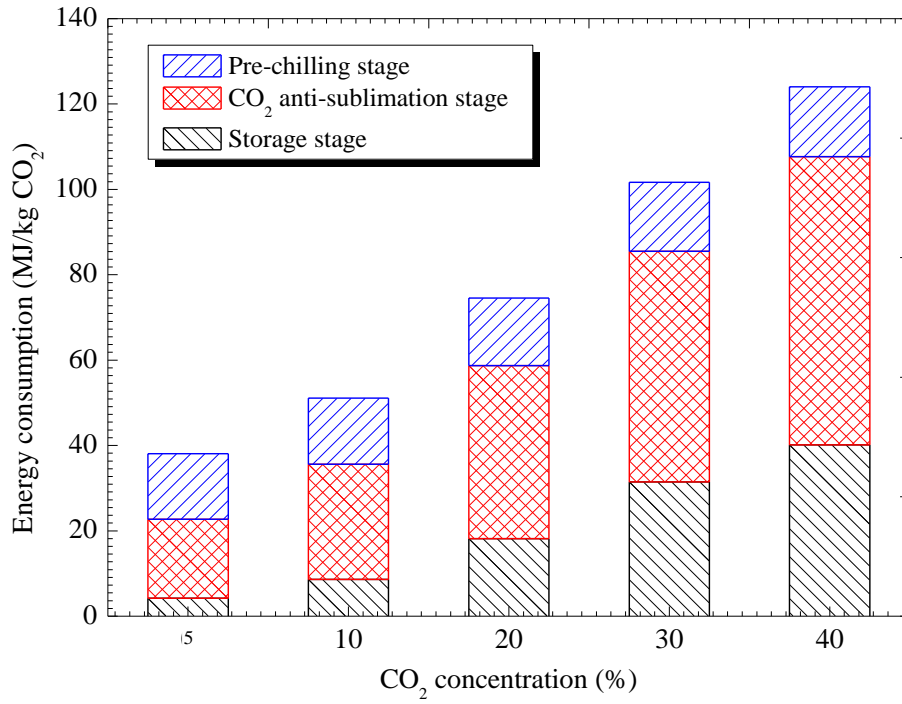
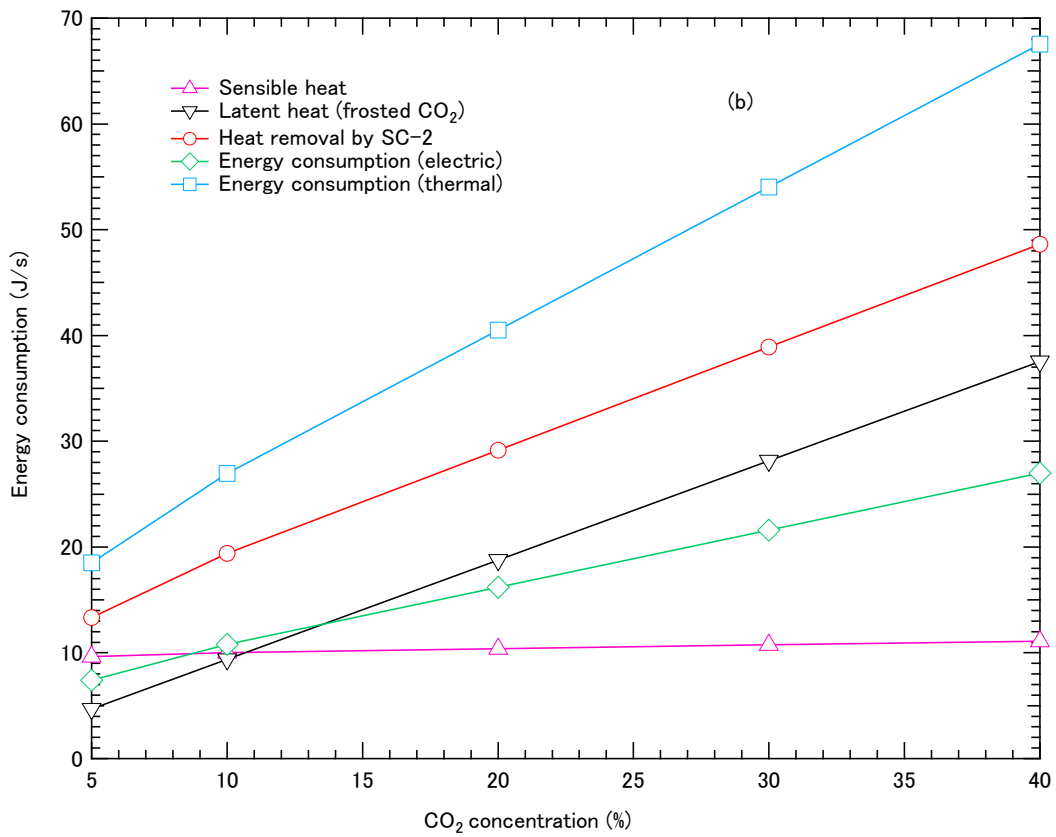
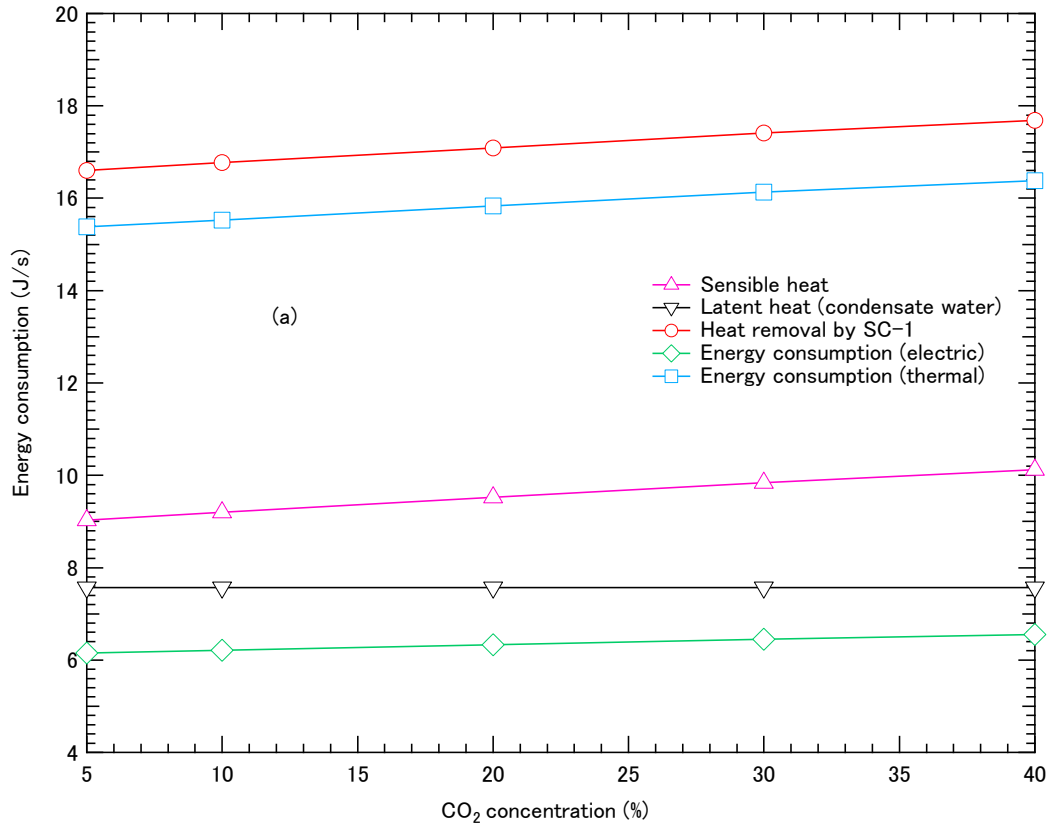


Fig. 11. Influence of CO₂ concentration on the energy consumption of the pre-chilling, CO₂ anti-sublimation and storage stages.



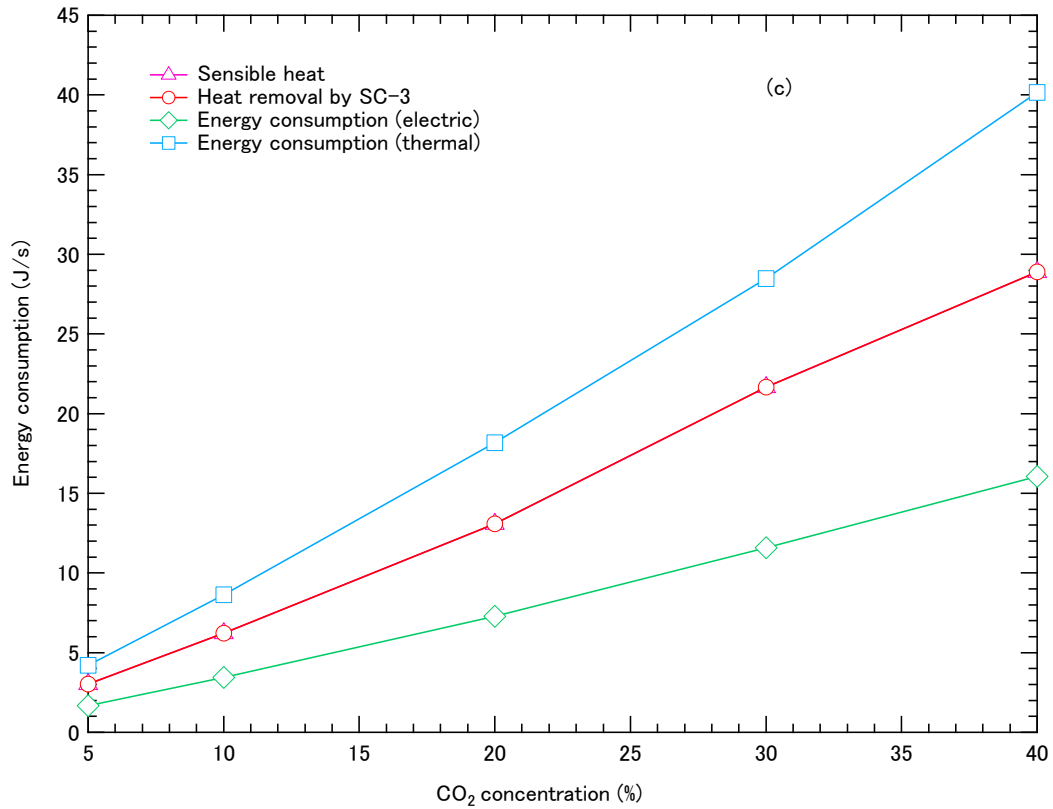


Fig. 12. Effect of CO₂ concentration on the energy consumption of the cryogenic CO₂ capture system. (a) Pre-chilling stage; (b) CO₂ anti-sublimation stage; (c) storage stage. The temperature of SC-1, 2 and 3 are set at -30°C, -120°C and -120°C, respectively. The COP of SC-1, 2 and 3 are 1.1, 0.7 and 0.7, respectively. The flow rate of flue gas is set at 5 L/min. The conversion efficiency from electric power to thermal energy is defined as 40%.

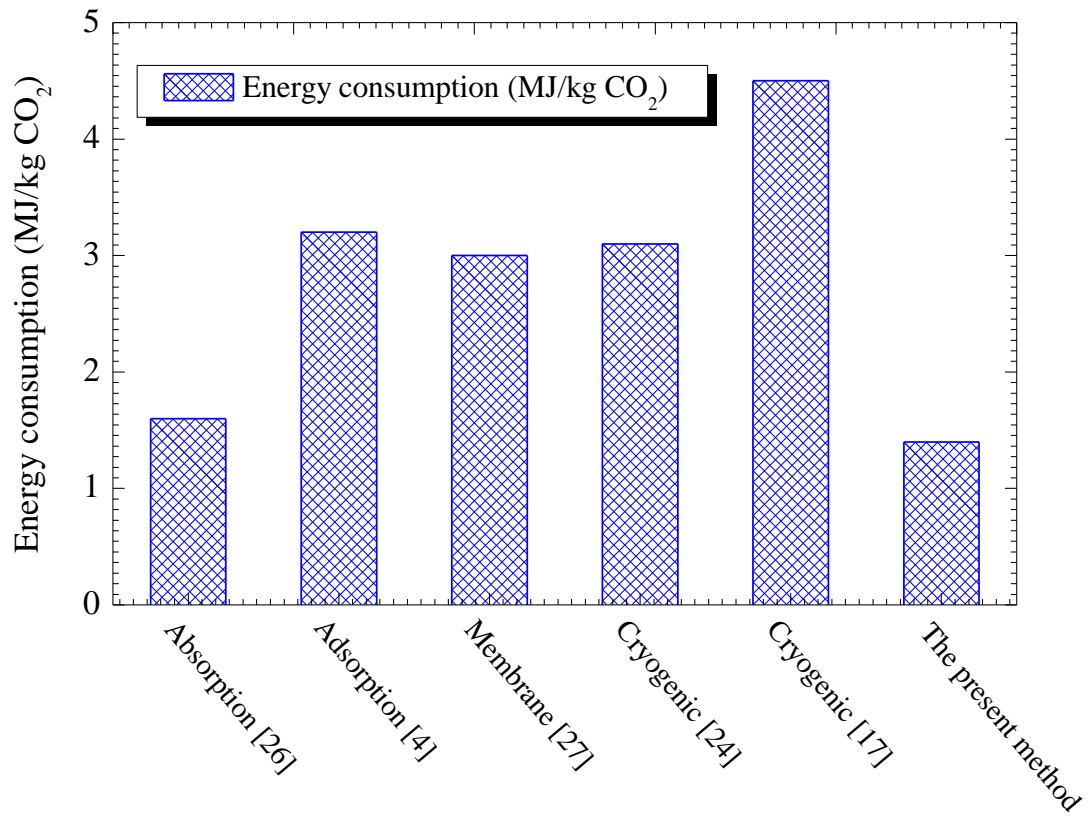


Fig. 13. Comparison of the existing CO₂ capture technologies.

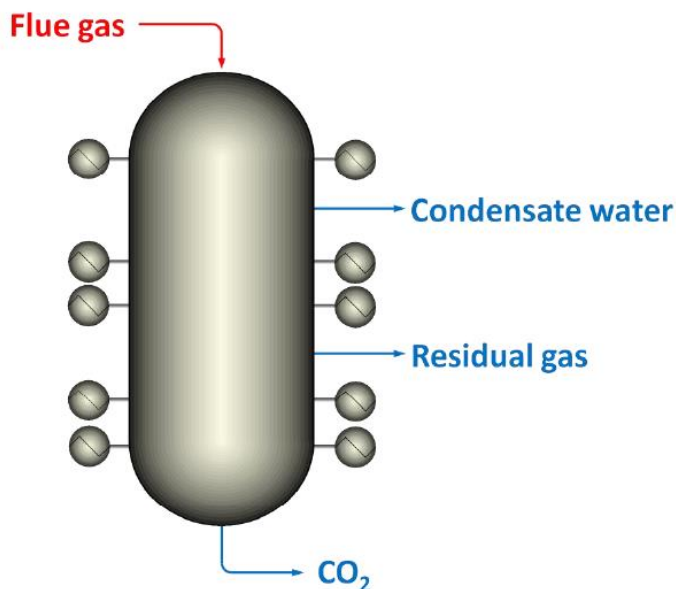


Fig. 14. Conceptual design of the scaled up cryogenic CO₂ capture process based Stirling coolers.

Table 1

Geometric dimensions of the three columns in the system.

Column	Geometric dimension (m)		
	OD*	ID*	L*
Pre-chilling	0.21	0.20	0.25
CO ₂ anti-sublimation	0.21	0.20	0.25
Storage	0.12	0.10	0.12

* OD, ID and L represent outside diameter, inside diameter and length of the column.

Table 2

Properties of the simulated flue gas (in a typical coal-fired power plant).

Properties	Value
Temperature	50 °C
Pressure	1.01×10^5 Pa
Composition of the feed gas	vol. %
CO ₂	13
N ₂	82
H ₂ O	5
SO _x	-
NO _x	-
Fly ash	-
CO ₂ recovery ratio	95 %
CO ₂ purity	99 %

Table 3

Parameters that influence the energy consumption of the system.

Parameters	Levels				
	#1	#2	#3	#4	#5
Temperature of SC-1 (°C)	-20	-30	-40	-50	-60
Flow rate of flue gas (L/min)	1	2	3	4	5
CO ₂ concentration (vol.%)	5	10	20	30	40

Table 4

Performance of the Stirling cooler (SC).

Performance	Stirling cooler
Power input	150 w
Cooling capacity	120 w (cold side temperature: -25 °C)
	50 w (cold side temperature: -80 °C)
	20 w (cold side temperature: -120 °C)
Frequency	≤10μm (peak to peak)
Working gas	Helium

Table 5Technical and economic evaluation of the cryogenic CO₂ capture system.

Section	Equipment	Capital cost (\$)	Operational cost (\$/h)
Pre-chilling tower	FPSC-1	3750	0.03
CO ₂ anti-sublimation tower	FPSC-2	3750	0.056
	Scraper	300	0.0045
Storage tower	FPSC-3	3750	0.056
Others	Control panel	12500	0.019
	Frame	37500	-
Total direct investment	6.16×10 ⁴		
Total operational investment	2.79×10 ⁴		
Total fixed investment	8.95×10 ⁴		
Capture performance			
CO ₂ recovery	90%		
CO ₂ purity	99.9%		
Energy consumption	1.37 MJ _{thermal} /kg CO ₂		
Capture cost	35 \$/kg CO ₂		

* The reference flow rate of gas mixture is 5 L/min.

Table 6

The boundary condition of the compared CO₂ capture technologies.

Properties	Absorption [26]	Adsorption [4]	Membrane [27]	Cryogenic [24]	Cryogenic [17]	The present work
Scale	600 MWe coal fired power plant	Laboratory	600 MWe coal fired power plant	Pilot plant	600 MWe coal fired power plant	Laboratory
Composition (vol. %)						
N ₂	86	90	87	81.4	86.5	82
O ₂	-	-	-	7	-	-
CO ₂	14	10	13	11.6	13.5	13
H ₂ O	-	-	-	-	-	5
Flow rate (kg/s)	666	0.67	602	3.45	635	0.17
Temperature (°C)	30	20	30	50	150	25
Pressure (bar)	1	1	1	1	1	1